Drake, L. (2016), Portable XRF: A (very) brief introduction. In: Homem, P.M. (ed.) *Lights On… Cultural Heritage and Museums!.* Porto: LabCR | FLUP, pp.140-161

PORTABLE XRF: A (VERY) BRIEF INTRODUCTION

Lee Drake[1]

ABSTRACT The growth of portable x-ray fluorescence instruments (pXRF) have challenged traditional analytical protocols, primarily in its use in non-destructive contexts.

The present manuscript evaluates the ways that pXRF differs from traditional laboratory XRF, and the limitations and opportunities which emerge from this difference. Both qualitative and quantitative uses are illustrated with a focus on applications for cultural heritage management.

KEYWORDS Portable X-Ray Fluorescence; Methodology; Qualitative; Quantitative

[1] Bruker, US, University of New Mexico, US, lee.drake@bruker.com

Perception of visible light

The perception of colors, from the reds of the thin, subtle smile in Da Vinci's Mona Lisa to the blue sky of Picasso's Starry Night, owe a debt to the evolution of our primate ancestors. While most mammals can clearly see blue and red, the ability to differentiate lower-energy/longer wavelength colors is rare. In the deep past, the primate ancestors of humans were dependent on differentiating red from green to find fruit in dense jungle stands - this created a powerful selective force which gave primates a broader spectrum than most other mammals (Regan et al. 1998). As can be seen in FIG. 1, the long and medium cone cells, responsible for red and green, have very subtle differences in sensitivity to different photon energies, as can be seen in FIG. 1. Our ability to see green may be due to a gene duplication event with some mutation that formed the M-cone from the L-cone (Nathans and Thomas, 1986).

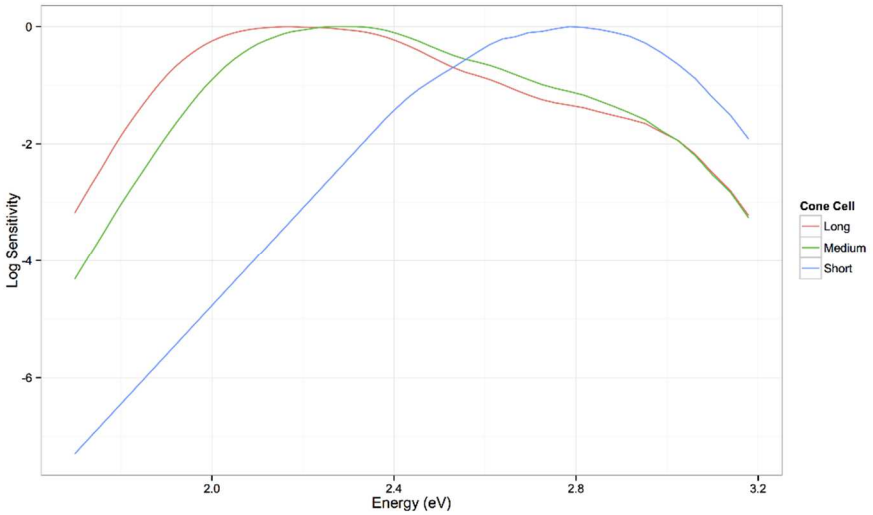

FIG. 1 - Cone cell energy sensitivity (Stockman et al., 1993).

Despite the closeness of energy sensitive, the eyes of modern humans are generally capable of differentiating between multiple hues between red and green, giving the world, and art, its richness of experience. It is important to underline here that the color range of humans, which extends from 1.7 to 3.1 electron volts (eV) of energy

(700 - 300 nanometers), is a product of our unique evolutionary history. Our perception of the world is confined to these limits. Other organisms have colors which exceed the unusually broad and detailed spectrum humans enjoy; some species of honeybees can see into the ultraviolet (UV) range, while others such as snakes perceive in the infrared (IR) range.

Outside the visible spectrum

The developments in instrumental science over the past several decades have used increasingly sophisticated light generators and detectors to make the known entirety of light's spectrum available to humans for study, from radio waves with 100 km wavelengths (1.2398e-11 eV) to the gamma rays of supernova of 300 keV (0.0004 nm wavelength). As such, the concept of color expands dramatically when we consider these higher and lower energy photons.

Miniaturization of components have taken formerly large laboratory-confined instruments into smaller, handheld devices (Bostco, 2013). This displacement from the lab has led to the use of handheld instrumentation in contexts which present unique challenges and opportunities. This paper concerns itself primarily with handheld x-ray fluorescence (pXRF) spectrometers, however the principles of matrix effects and attenuation will affect other types of instrumentation as well.

XRF instruments (FIG. 2) attain their portability by using geometry to fit key components in small spaces. An X-ray tube is configured at a 52° angle relative to the nose of the instrument. This is not the best geometry of an XRF instrument, an angle of 90° is preferable for maximum limits of detection (Klockenkaemper, 1997). However, the

geometry is key for portable instrumentation to work, and this is one sacrifice to a smaller system. Photons edited from this angle will strike the sample and excite atoms within it. Emitted photons from the sample will then strike the detector which is set at a glancing angle. The detector functions in the same way as cone cells do in the human eye; they identify the energy of a photon.

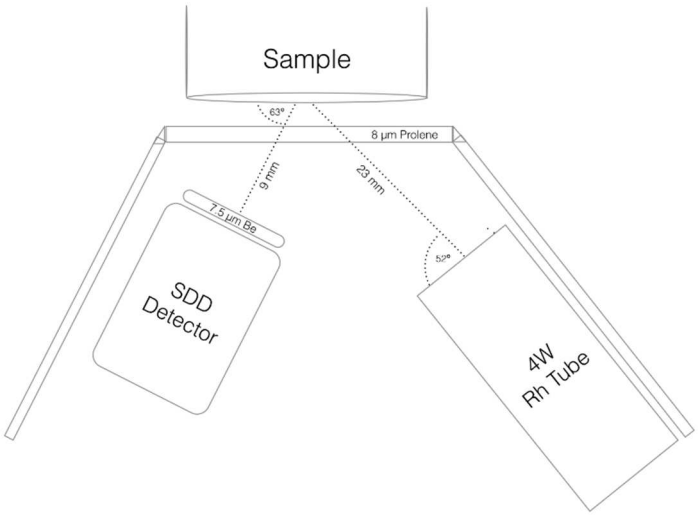

FIG. 2 - Configuration of typical handheld XRF instrument (Bruker Tracer IIISD).

X-ray fluorescence (XRF) as a process concerns itself with the fluorescence of elements. These energies range between 0.3 and 100 keV, though most XRF or similar instruments analyze only a portion of that range. Physically, they operate based on the same principles as visible color, an incoming photon excites an electron, and causes disorder in the electron shells. As the electrons re-align, they emit new photons which represent the energy residuals of their transitions within the atom. For color fluorescence, this typically takes place in the shared outer electron shells of molecules; with XRF this occurs internally to the atom, in the M, L, and K shells closest to the nucleus. The typical spectrum includes characteristic lines (FIG. 3):

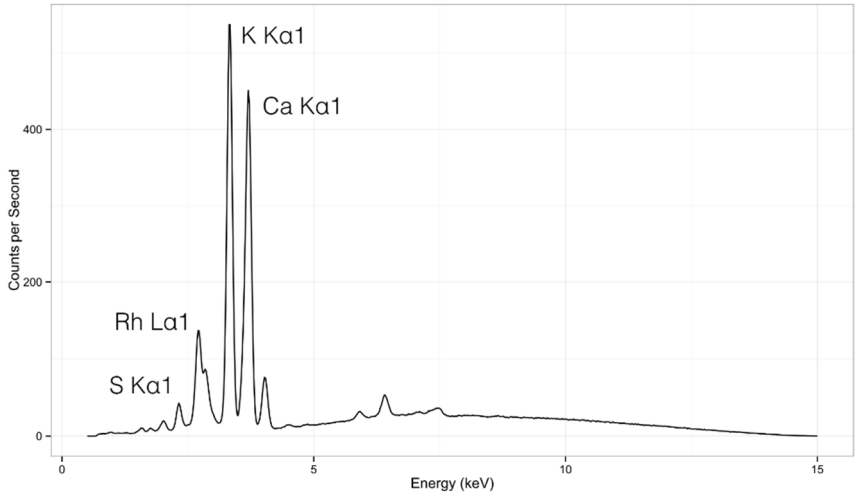

FIG. 3 - XRF spectrum of NIST 1547, Apple Mango Leaves.

In this case, each element fluoresces with unique peaks - Potassium (K) has a K-alpha line at 3.55 keV, and a K-beta peak at 3.60 keV. These can be thought of as the colors of Potassium, if red is 1.7 eV and blue 3.0 eV, then Potassium's K-alpha line is a color at 3,550 eV.

Again, the XRF spectrum is an extension of our color vision, something which enables us to see more than the colors our primate ancestors left us with. The big difference is what we see - with visible color fluorescence it is the molecules which fluoresce. For example, reduced iron (Fe^{2+}) looks black to us, because all visible photons are absorbed. If it is oxidized to hematite (Fe_2O_3) then we would see an orange-red color. This is because photons of an energy of 1.7 - 1.9 eV are emitted from the shared outer electron shells of the molecule following light's absorption.

To an XRF unit, the Fe K-alpha and K-beta lines (6.4 and 6.9 keV, respectively) would fluoresce just the same - the arrangement in the outer electron shells does not affect the absorption or emission energies of those orbitals closest to the nucleus. As such, XRF is primarily a method to detect elements.

The XRF spectrum

The XRF spectrum is most typically used in the identification and/or quantification of elemental fluorescence peaks. However, there are multiple other types of photon interaction present than simple fluorescence.

In FIG. 4, numerous other peaks manifest in the spectrum. These include the Rayleigh peak, which is formed by elastic scatter of photons from the XRF tube. These will have an energy that matches the K-alpha (or L-alpha) line of the x-ray target.

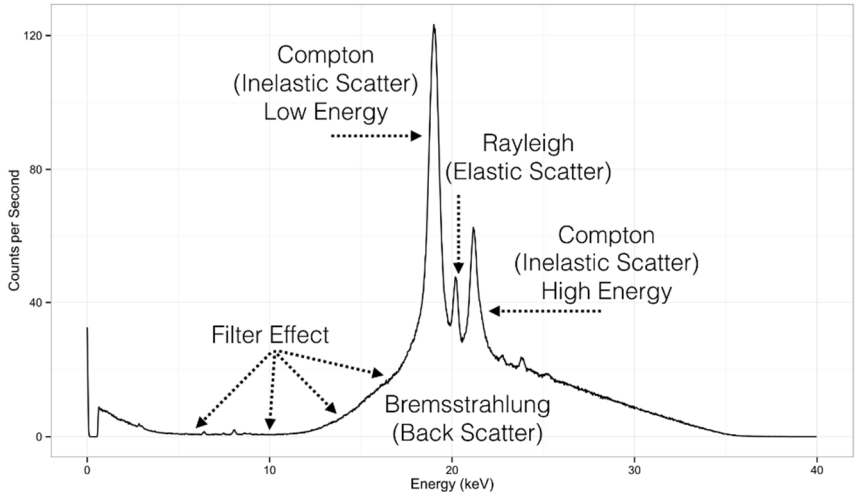

FIG. 4 - Spectrum of a diamond taken with a 25 µm Ti/300 µm Al filter and a rhodium (Rh) tube.

They are formed when photons leave the tube and are reflected by the sample without losing any energy - they are the parallel for white light in this portion of the spectrum. The Rayleigh peak is situated between two Compton peaks, one at a lower energy at another at a higher energy. These are the inelastic scatter that results from photons with the energy of the XRF target (e.g. same as Rayleigh) but they loose (or gain) energy on their way back to the detector. The ratio of the lower-energy Compton peak to Rayleigh will correspond to the density of the electron cloud (e.g. higher ratio with lighter elements). These three peaks overlay a broader set of photon counts, collectively known as Bremsstrahlung radiation. These are the x-ray photons which simply

bounce around in the matrix of the material and loose energy - they are informally known as the backscatter. To the left, the backscatter does not mirror its counterpart to the right, it has a bowl-curve descending to 0 counts per second. This is the consequence of adding a filter, which eliminates a portion of the spectrum. This is typically done to increase the signal-to-noise ratio of elements with fluoresce in a given region.

Peaks fluoresce in the spectrum based on the quantity of atoms present and the luminescence settings of the instrument used. Just as with color fluorescence, more energy must be sent than is returned. Each element has a range of photons which can excite electrons in its K, L, and M orbitals. There is a terminal point at which a certain photon can no longer excite these orbitals for a given element, this is known as the absorption edge. This point is also the point of maximum excitation potential, the effectiveness of a photon to excite the element in question declines with higher energies. The overall potential of excitation looks something like a Gaussian distribution which was cut in half (FIG. 5).

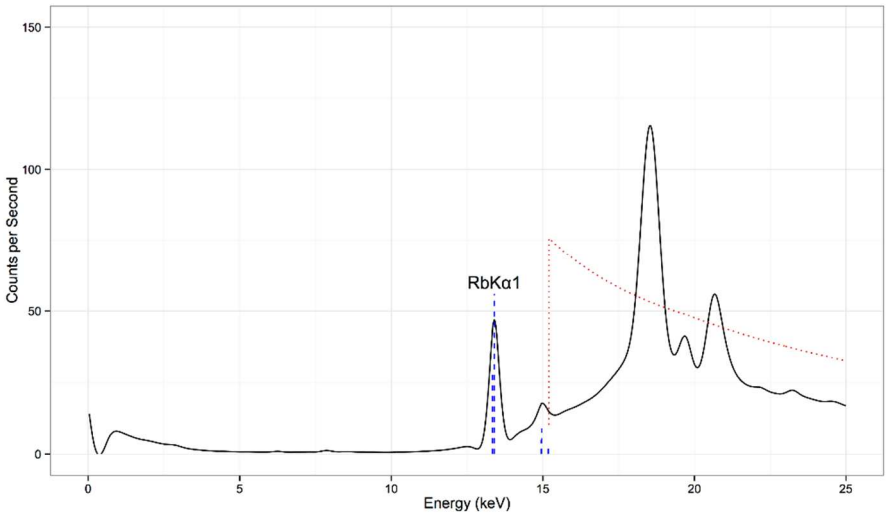

FIG. 5 - Absorption Edge of Rubidium (Rb).

The fewer photons there are to the right of the absorption edge, the smaller the chance of fluorescence there is. The converse is also true,

the more photons on the absorption edge, the higher the chance of fluorescence. Filters can be used to increase or decrease the chance of an element fluorescing, but ultimately the ability to seen an element rests with the sample.

What makes pXRF different?

For decades, laboratory XRF units have been highly reliable systems with straightforward quantification. However, portable XRF instruments are much more difficult to use quantitatively (Frahm, 2013). The components between the two are the same, why would portable XRF underperform? The reason has less to do with the configuration of the XRF and more to do with the sample. Laboratory XRF units typically analyze prepared samples, usually fused glass beads. This means samples have been homogenized and prepared for analysis - this also means the matrix (in this case SiO_2) matches that of the reference standards of the equipment. Portable XRF, in contrast, is used in situations where samples are not prepared. In fact, the use of pXRF is frequently on heterogenous samples. As such, the limitations stem not from the physical components but rather the use of the system to analyze paintings, ceramics, and other heterogenous objects in a non-destructive manner (Kaiser and Shugar, 2012). That said, when samples are prepared the same way, portable instrumentation can have equal performance to laboratory equipment (Guerra et al., 2014).

This means, in short, that matrix effects are essential considerations in the use of portable XRF. Some elaboration may be needed on the term matrix; this simply refers to the majority material by composition. The matrix of soil would be SiO_2, the matrix of stainless steel would be a

crystalline mixture of Fe, Cr, and Ni. The matrix affects the spectrum in two primary ways, the first is by affecting the depth of analysis.

The depth of analysis is the product of the mass attenuation of photons as they enter any matrix, be it gas, liquid, or solid. The atoms of the matrix gradually absorb photons. The denser the matrix, the more rapid this loss of photons is. Photons with higher energies will be able to make it further into the matrix. The relationship can be expressed as follows:

$$I/I_0 = e^{[-(\mu/\rho)\rho]}$$

where I is the quantity of photons returning from the sample, I_0 is the quantity of photons entering the sample, μ/ρ represents the mass attenuation coefficient of a given element for a particular matrix, and ρ represents the density of the object. Assuming only 1% of photons return from a sample, the equation can be reduced to:

$$\text{depth (cm)} = 4.61/(-\mu/\rho*\rho)$$

In this case, the depth of analysis for a silicate can be calculated (FIG. 6):

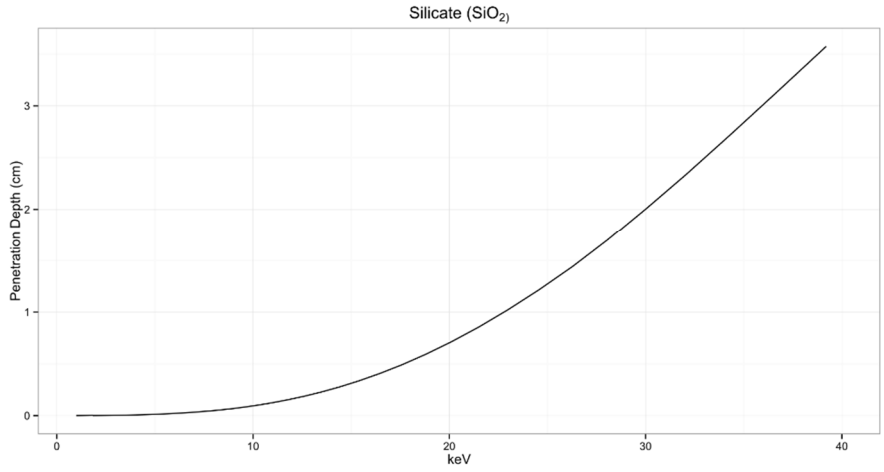

FIG. 6 - Depth of analysis for a silicate by photon energy.

For light elements, such as Si, the analytical depth is only 27 μm for the K-alpha peak. For heavier elements, such as the K-alpha emission for

Fe, it can be 300 µm deep. The L-line for Pb would be 1,130 µm, and Ag's K-alpha peak can be seen at a depth of over 200,000 µm, or 2 cm, deep. As such, the spectrum will produce a biased view of different elements depending on their energy.

Second, the presence of new elements can influence the fluorescence of others as they can overly each other's absorption edges.

In FIG. 7, Fe sits on the absorption edge of Ti, which in turn sits on the absorption edge of S.

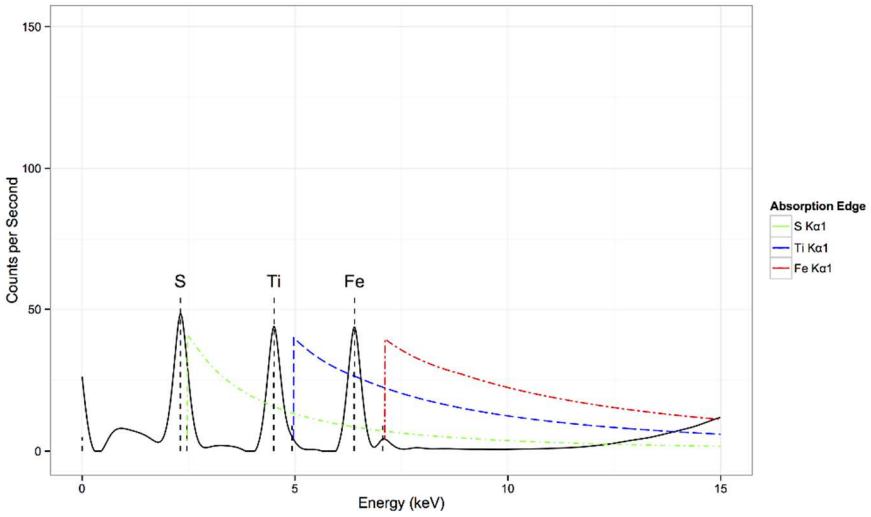

FIG. 7 - Absorption edges for S, Ti, and Fe.

In this case, each element heightens the fluorescence of an element of lower energy. And in turn, each element of lower energy reduced the height of the higher energy peak lying in its absorption edge. An Fe K-alpha photon can be emitted, then strike a Ti atom, which in turn emits a Ti K-alpha photon, which is absorbed by S. This highlights the resonance effect which takes place in elemental spectra. As an analogy, the spectrum can be thought of as a symphony, and each element an instrument. As the violins swell, the clarinet deepens. The user of portable XRF equipment can conduct analysis more effectively by shaping the energy, current, filter, and even atmosphere that the analysis is taken in to accentuate the fluorescence of elements.

As mentioned before, laboratory instruments also deal with these physical phenomenon, but in a controlled setting. They standardize the matrix, and can be calibrated to a higher degree. Portable instrumentation is much more vulnerable to matrix effects because the sample analyzed are typically heterogenous and unprepared. While this is a sacrifice from the point of view of spectrum quality, it is an advantage in that it is non-destructive. A painting can be painlessly analyzed using XRF, while in most cases the homogenization of the pigments into a fused glass bead are unpalatable. It is important to note, in non-destructive uses of the equipment, that matrix effects not be taken for granted. It is important for spectra to be assessed qualitatively given these conditions.

Qualitative analysis

The utility in art conservation for XRF consists in expanding our spectrum to see those elements which are compositionally important to a piece of art or a heritage object. For conservation, XRF can be used to identify elements or materials which may not be consistent with the point of origin of an object, identifying potentially reactive elements, or to analyze variation in the composition, among other tasks. In general, any analysis first needs context. For example, analysis of a historical painting means that a certain set of pigments are expected for its point of composition. A Rembrandt painting will include historical pigments such as lead white ($PbCO_3$), vermillion (HgS) and bone black ($CaPO_4$) based on their availability during the time in which he was alive. If a synthetic pigment base such as titanium dioxide (TiO_2) or zinc oxide (ZnO) is present, then the painting is either retouched, or is not secure in its provenance. Likewise, the identification of calcite ($CaCO_3$) or gypsum ($CaSO_4$) could indicate the presence of the recent,

reversible restoration. In either case, the context of the object is inseparable from the interpretation of XRF spectra - neither exists in isolation.

A similar example can exist with heritage objects. In North America, pre-Colombian cultures rarely used anything other than pure copper or gold as metals. An XRF spectrum of these objects should produce pure K lines for Cu or L lines for gold, with the potential for small impurities like Ag and Pb. The presence of a substantial amount of Zn or Sn would indicate a brass or bronze alloy, technology with had no president prior to the arrival of the Spanish in 1492.

Note that in these two examples XRF does not need to be used quantitatively to answer a straightforward question: do we understand the object's place in time? Qualitative analysis is sufficient to answer this question. The qualitative analysis of XRF spectra is, in essence, the same as qualitative analysis performed with human eyes - no further elaboration is always needed when describing a color such as red. In the same sense, no further elaboration is needed when a brass object shows up in a prehistoric collection - it is impossible for it to be both brass and prehistoric.

Complications to qualitative analysis

The intensity of the K-, L-, and M- peaks in an XRF spectrum corresponds to the relative abundance of that element give the fluorescence parameters (energy, filter, atmosphere, etc.). The spectral peaks can be thought of as proxies for atoms themselves, though there are some basic factors that complicate this picture (FIG. 8).

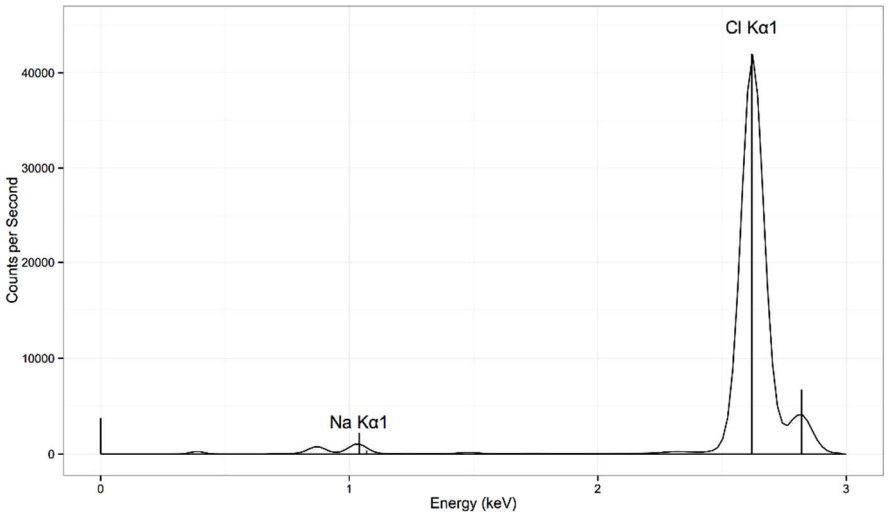

FIG. 8 - Spectrum of sodium chloride taken using a helium flush. The small peak to the left of the Na K-alpha peak is the escape peak for Cl.

By atomic abundance, sodium chloride is 50% Na and 50% Cl. So, why is the Cl K-alpha peak magnitudes of order higher than the Na peak? There are three reasons why:

1. The depth of analysis of Cl is 38 µm, while Na is 5µm;
2. Cl is closer to the medium of the Brehmsstralung radiation, while Na at the tail;
3. Cl has a fluorescence efficiency of 9%, while Na has a fluorescence efficiency of 2%.

As such, there are few photons to fluoresce Na, which in turn fluoresces less efficiently, and at a shallower depth than Cl. These factors combine to dramatically reduce the Na K-alpha peak. The first two factors have been covered earlier in this manuscript, the latter is in need of further elaboration. Fluorescence efficiency refers to how many atoms out of 100 will fluoresce in a given electron orbital if a photon has the necessary energy. This efficiency is determined by the number of electrons in the outer orbitals and the repulsive charges they have on each other. A lower number means less atoms will light up; a higher number means more. Typically, the more electrons in the outer orbitals, the more likely a K-alpha or L-alpha emission will occur.

Because Na is a lighter element than Cl, there are less candidates for the transfer.

For these reasons, the spectral peaks cannot be considered perfect proxies for atomic counts - there are many biases at work that affect the fluorescence of elements, not all of which can be controlled by the user. That said, if fluorescence parameters, or illumination, is kept constant from sample to sample (e.g. same energy, current, filter, time, and atmosphere) then peaks of the same element in different samples will vary based on their concentrations/atomic abundances.

Quantitative analysis

Typically, we tend to think about the presence of elements in material in terms of concentrations, e.g. 7% Fe, 325 ppm Rb. These percentages refer to either volume or, more commonly, weight. However, the use of weight percent to characterize material can sometimes obscure its composition somewhat. Take our earlier example of salt. It is 50% Na and 50% Cl by atomic abundance, captured by its chemical formula NaCl. However, Na has 11 protons while Cl has 17. This means that Na has an atomic weight (with common isotopes included) of 22.99 while Cl has one of 35.45. Cl thus weights 54% more than Na. As such, NaCl is by weight 39% and Cl 61%. Think about the contradiction there for just a moment - while there are just as many atoms of Na and Cl in salt the latter is a greater weight percent than the former. Phrasing composition in the context of weight conflates two different points of variation - the atomic abundance of an element and its atomic weight. A more dramatic example can be seen with water, H_2O. H has an atomic weight of 1 while O has an atomic weight of 16. There are twice as many H atoms as there are of O, yet those H atoms compose roughly 11% of water's weight.

The prominence of weight % in chemical composition analysis owes to the history of chemistry. In the classical and medieval eras, there were two major branches of chemistry, the first being alchemy (the attempts to transform elements into gold) and the second being metallurgy (the process of creating tools, weapons, and structures). Both carefully weighed out ingredients prior to incorporation into materials and experiments. For example, a metallurgist would add 1 kg Sn for every 9 kg Cu to create a bronze sword. This tradition carried over into modern material science in most cases, remaining the standard by which we analyze objects today.

From the perspective of XRF, a major complication is added - the traditional units of composition are not directly reflected in the atomic spectrum. To perform quantitative analysis - specifically in terms of weight percent - some kind of calibration is needed. There are two primary mathematical approaches to doing this. The first is to use fundamental parameters of the instrumentation to create estimates of an item's composition. This includes the angle of the x-ray tube, the glancing angle of the detector, the space from the sample to the detector, and assumptions about composition. If dealing with a sample in which 100% of the atoms fluoresce in range of the tube and detector's capabilities, this approach can work quite well because all points of variation can be included. If, however, not all elements can be seen, then the situation becomes much more complicated. For example, a piece of glass is, by both weight and volume, mostly O. EDXRF cannot detect this element - even if it could it would only be at a depth of 10 nm in the sample. FP algorithms must from this point make a guess about the elements it cannot see to estimate the weight percent of Fe, Cu, Zn, and other metals. The inability to see Na without atmospheric changes further complicates the task. Though glass

represents a partially synthetic material, SiO_2 and Al_2O_3 are dominant and oxygen can be extrapolated from there. Soils and ceramics are much more challenging. There are multiple forms for Ca, including $CaSO_4$, $CaPO_4$, CaO, $CaCO_3$, etc. There are two common oxidization states for Iron, Fe_2O_3, FeO, etc. FP algorithms work best with highly synthetic substances such as metals in which all elements present can be excited by the instrument. An example is the Rosseau (2009) FP algorithm:

$$C_i = R_i ((1 + \Sigma_j A_{ij} C_j)/(1+\Sigma_j \varepsilon_{ij} C_j))$$

where C_i represents the concentration of an element, R_i is the relative intensity of an element, a_{ij} are the absorption coefficients, C_j represents the element at concentration, and ε_{ij} represents the enhancement coefficients. Determination of a_{ij} and ε_{ij} require information on total matrix composition - thus the algorithm only functions if a prior is given to it (e.g. information about the sample). For proper FP calculation, additional information about the tube and detector geometry/distance is needed, such as those details documented in FIG. 2.

The second major method to quantify XRF spectra is to use reference standards, these are known as empirical calibrations. The approach of an Empirical calibration is most commonly a variant of the common linear model developed by Lukas-Tooth and Price (1961):

$$C_i = r_0 + I_i(r_i + \Sigma r_{in} + I_n)$$

Where C_i represents the concentration of element, r_0 is the intercept/empirical constant for element i, r_i - slope/empirical coefficient for intensity of element i, r_n is the slope/empirical constant for effect of element n on element i, I_i is the net intensity of element I,

and I_n is the net intensity of element n. This equation descends from a simple linear model,

$$y = mx + b$$

In which y is C_i, b is r_0, m is r_i, and I_i is x (eg. $C_i = r_i I_i + r_0$). The additional variables present in the Lukas-Tooth equation indicate a slope correction for an element which influences the fluorescence of the element to be analyzed (subscript i represents the element being analyzed, subscript n represents the influencing element). An illustration of how this effect occurs can be seen in FIG. 7. Here, the K-alpha peak of Fe overlays the absorption edge for the K-alpha emission of Ti. In this circumstance, the quantification of Ti may use Fe as a slope correction. While the Lukas-Tooth method of quantification has been criticized for being a brute-force statistical quantification approach, physical principles can be used to guide the application of corrections. It is important, however, to strive for minimalism in these quantifications. Too many corrections can artificially increase the r^2 value of a linear/non-linear model. Unrelated corrections will inflate the perceived accuracy of the model; real world application will increase the chance of a violation to its generalizability. The fewer corrections, the more generalizable the model. An additional benefit is that violations to a simple Empirical Calibration can result in systematic error as opposed to random error (Nazaroff et al., 2010).

By using matrix-specific calibrations, almost any material can be quantified using EDXRF data (Speakman and Shackley, 2013). FIG. 8 shows a simple empirical calibration built for ppm-levels of Pb in water in this case, 10,000 ppm of a reference standard (Lead, 10,000 ppm, ICP Standard Solution) was titrated down to 1ppm using repeat half-dilutions with distilled water (FIG. 9).

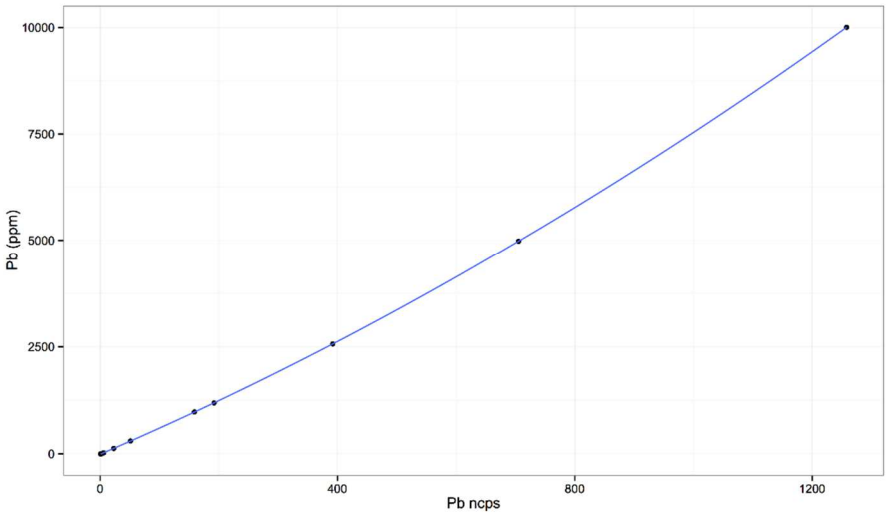

FIG. 9 - Pb in water empirical calibration.

This calibration represents the simplistic possible implementation of a calibration, in which there are no overlapping peaks. Note that even in this case the effect is beyond a simple linear model; a quadratic formula was used due to the effects of depth on the analysis. Calibration curves become more complicated as different overlapping elemental lines influence the curve. The Lukas-Tooth and Price equation will turn these into multilinear models - thus creating multi-dimensional calibration curves that cannot easily be displayed in a bivariate plot. Nonetheless, the principles are simple and straightforward.

Layer thickness and position

XRF has one highly unique application in which non-destructive analysis provides more detailed information than simple concentrations. In the right circumstances, it can be used to predict the thickness of an object with micron-level accuracy. This is a consequence of two factors in XRF; the first is that there are multiple peaks for each element at different energies, the second is that higher energy photons penetrate greater depths of a material. To return to

the example of Pb, it has two primary L peaks, an L-alpha at 10.5 keV and an L-beta at 12.5 keV. The attenuation of the L-alpha peak will be greater in every matrix than the L-beta since it has 20% less energy. This means that as the L-beta peak rises relative to the L-alpha peak, the depth of the surface covering must also increase. FIG. 10 illustrated this effect with different thicknesses of pure Al foil, ranging from 0 to 775 µm Al overlaying pure Pb.

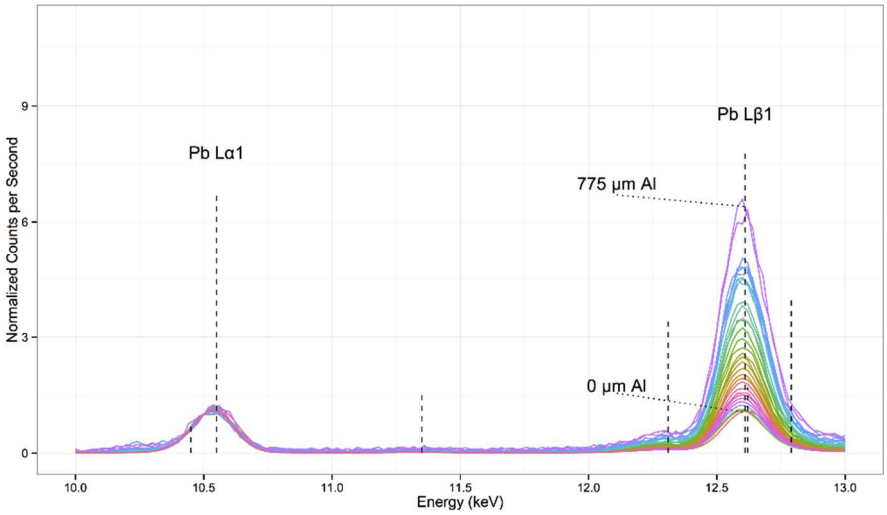

FIG. 10 - Pure Pb covered with increments of 25 µm of Al; as the Al layer gets thicker, the Pb L-beta/Pb L-alpha ratio gets larger.

This principle can be used to identify surface coverings - indeed an entire industry of coating thickness analyzers exists based on this principle. The same principle holds true for any conceivable layering; varnishes on a painting, pigments on top of other pigments, metal plating on other metal. The analysis can be done spectrally, provided that a surface-level reading of the low layer is available. An example of this is the spectrum of Pb in Figure 9: The smallest L-beta represents the surface-level measurement of Pb; the L-beta/L-alpha ratio here is about 0.85. By contrast, the L-beta/L-alpha ratio for Pb beneath 775 µm of Al is 4.92; in other words, the L-beta peak went from being 85% the size of the L-alpha peak to being 492% larger. It is important to note that it is not the case that the L-beta peak is getting bigger - rather it is simply shrinking less quickly. 775 µm Al shrunk the L-alpha peak by

96.5%, while only striking the L-beta peak by 80%. It is resistance to attenuation that creates this effect.

One important word of caution, the above application assumes that there are no independent influences on the fluorescence of Pb. As noted earlier in this manuscript, absorption edges are an important secondary influence on the fluorescence of an emission line. A spectrum should be screened qualitatively for overlapping elements on the absorption edge of the target element.

Summary

XRF is most commonly used as a laboratory technique for determining concentrations, this has been the primary interaction with the technology for decades. The rise of portable, non-destructive instrumentation has challenged many researchers - how to make this technology work in circumstances in which samples are heterogenous? But with every challenge comes an opportunity if one can interpret the spectrum properly.

The present manuscript focuses on a few important spectral effects and guidelines for interpretation. There are many more ways to use XRF as either a qualitative or quantitative tool, but the first step is in the spectrum. Further analysis, qualitative, quantitative, or otherwise, follows from it.

References

Bosco, G.L. (2012), Development and application of portable, hand-held X-ray fluorescence spectrometers. *Trends in Analytical Chemistry*, 45: pp.121-134.

Frahm, E. (2013), Validity of "Off-the-Shelf" handheld portable XRF for sourcing near eastern Obsidian chip debris. *Journal of Archaeological Science*, 40(2).

Guerra, M.B.B.; de Almeida, E.; Carvalho, G.G.A.; Souza, P.F.; Nunes, L.C.; Santos, D., Krug, F.J. (2014), Comparison of analytical performance of benchtop and handheld energy dispersive X-ray fluorescence systems for the direct analysis of plant materials. *Journal of Analytical Atomic Spectroscopy*, 29, pp.1667-1674.

Kaiser, B.; Shugar, A. (2012), Glass analysis utilizing handheld X-ray fluorescence. In Shugar, A. & Mass, J.L. (eds), Handheld XRF for Art and Archaeology. Leuven, BE: Leuven Press, pp.449-470.

Klockenkaemper, R. (1997), Total-Reflection X-ray Fluorescence Analysis, New York: Wiley.

Lucas-Tooth, H.J. & Price, B.J. (1961), A Mathematical Method for the Investigation of Interelement Effects in X-Ray Fluorescence Analysis *Metallurgia,* 64, pp.149–152.

Nathans, J. & Thomas, D. (1986), Molecular genetics of human color vision: the genes encoding blue, green and red pigments. *Science*, 232 (4747): pp.193–203.

Nazaroff, A.J.; Prufer, K.M.; Drake, B.L. (2010), Assessing the applicability of portable X-ray fluorescence spectrometry for obsidian provenance research in the Maya lowlands. *Journal of Archaeological Science,* 37: pp.885-895

Regan, B.C.; Julliot, C.; Simmen, B.; Viénot, F.; Charles-Dominique, P., Mollon, J.D. (1998), Frugivory and colour vision in Alouatta seniculus, a trichromatic platyrrhine monkey. *Vision Research,* 38(21): pp.3321-3327

Rosseau, R.M. (2009), The quest for a fundamental algorithm in X-ray fluorescence analysis and calibration. *The Open Spectroscopy Journal*, 3: pp.31-42.

Speakman, R.J.; Shackley, M.S. (2013), Silo science and portable XRF in archaeology: a response to Frahm. *Journal of Archaeological Science,* 40: pp.1435-1443.

Stockman, A.; MacLeod, D.I.A.; Johnson, N.E. (1993) Spectral sensitivities of the human cones. *Journal of the Optical Society of America A,* 10(12): pp.2491-2521.